Modeling the Dynamic Processing of the Presynaptic Terminals for Intrabody Nanonetworks

Angela Sara Cacciapuoti, *Senior Member, IEEE*, Alessandro Piras, and Marcello Caleffi, *Senior Member, IEEE*

***Abstract*—Experimental evidences show that: 1) the release sites from a single axon have variable release probabilities, even when the axon contacts the same postsynaptic neuron; 2) this variability in the release probability implies a compartmentalization at the level of the presynaptic terminals of the neuronal processing; 3) the specificity of the presynaptic terminal processing is driven by and reflects the complex biophysical mechanisms activated at the axon terminals when a spike is fired in response to a stimulus. Stemming from these experimental evidences, we propose a communication engineering model for capturing the behavior of biological neurons. Specifically, by adopting a stochastic approach, the presynaptic terminals are modeled as a dynamic array of transmitters, where each transmitter models the processing specificity of a presynaptic terminal. In particular, we first show that the unique and specific processing of a presynaptic terminal can be reconducted to the cascade of a frequency selector and an amplitude modulator. Then, we characterize the propagation of the presynaptic-filtered signal through the synaptic cleft, and we derive the delay along with the channel attenuation as a function of the distance between the communicating neurons. Finally, the theoretical analysis is validated through numerical simulation.**

***Index Terms*—Neuro-spike communications, neurons, intrabody nanonetworks.**

I. Introduction

RECENT developments in nanotechnology and communication engineering are enabling the realization of a new generation of nanoscale devices implantable inside the human body [1], [2]. When interconnected in a network, referred to as *Intrabody nanonetwork* [3], [4], these miniaturized devices or nanomachines are able to perform complex tasks, by overcoming their individual limitations.

Recently, intrabody nanonetworks have been proposed for monitoring the human nervous system [5]–[7] by exploiting the dimensional similarity of the nanomachines with the nervous biological structures. The aim is to develop radically new medical diagnosis and treatment techniques. However, several questions and challenges arise to design a fully functional intrabody nanonetwork deployed inside the nervous system. Certainly, the first step is to understand the physiological mechanisms underlying the neuronal activities with an engineering perspective for mapping such mechanisms into communication engineering system models [8]–[10].

The communication models available in the literature consider the axon terminals[1] acting solely as stochastic conveyers of information through the synapses[2] from a neuron, referred to as presynaptic neuron, to a targeted neuron, referred to as postsynaptic neuron. However, this model is too simplistic. Indeed, a very large number of evidences from experimental studies [11]–[15] conducted on biological neurons show a high compartmentalization at level of individual axon terminals of the neuronal processes. This compartmentalization in turn implies that the axon terminals act as unique dynamic signaling units, whose effects on the transmitted signal from a presynaptic neuron to a postsynaptic neuron, can vary enormously depending on the activity history at either or both sides of the synapse [14].

Specifically, numerous experiments have shown that the processing specificity of an axon terminal is a universal property and potentially unique for each synaptic connection made by a single axon [12], [14], [15]. In fact, it is determined by the unique interaction between the pre- and the postsynaptic neurons. More in detail, the axon-terminal-specific processing is due to and reflects the complex biophysical mechanisms activated at the axon terminals by the electrical signals, known as action potentials (APs) or spikes, fired in response to a stimulus. So, when an AP reaches different axon terminals, the axon-terminal-specific processing determines different patterns of neurotransmitter release. As a consequence, a presynaptic neuron simultaneously transmits different signals to a postsynaptic neuron, and not just a single signal. Collectively, knowing which axon terminal releases neurotransmitters provides more information than simply knowing that a neuron has fired [12], [14], [15].

Stemming from these experimental evidences, it is clear that an effective neuronal communication model should take into account the processing dynamics of the axon-terminals, in the following referred to as *presynaptic terminals*[3]. Hence, in this paper, a communication engineering model is designed for capturing the behavior of biological neurons, by accounting for

Manuscript received July 30, 2015; revised December 23, 2015; accepted January 15, 2016. Date of publication January 21, 2016; date of current version April 13, 2016. This work was supported in part by the PON projects "FERSAT: studio di un sistema di segnalamento FERroviario basato sull'innovativo utilizzo delle tecnologie SATellitari e della loro integrazione con le tecnologie terrestri" and DATABANC "CHIS: Cultural Heritage Information System," and in part by the Campania POR project "myOpenGov." The associate editor coordinating the review of this paper and approving it for publication was M. Pierobon.

A. S. Cacciapuoti and M. Caleffi are with the DIETI Department, University of Naples Federico II, Naples I-80125, Italy (e-mail: angelasara.cacciapuoti@unina.it; marcello.caleffi@unina.it).

A. Piras is with Consorzio Nazionale Interuniversitario per le Telecomunicazioni (CNIT), Naples 80126, Italy (e-mail: apiras@cnit.it).

Color versions of one or more of the figures in this paper are available online at http://ieeexplore.ieee.org.

Digital Object Identifier 10.1109/TCOMM.2016.2520476

[1]The axon terminals, or synaptic boutons, are the distal terminations of the branches of an axon, as illustrated in Fig. 1.

[2]The synapses are the junctions through which the neurons signal to each other.

[3]For a formal definition of presynaptic terminal please refer to Section II.

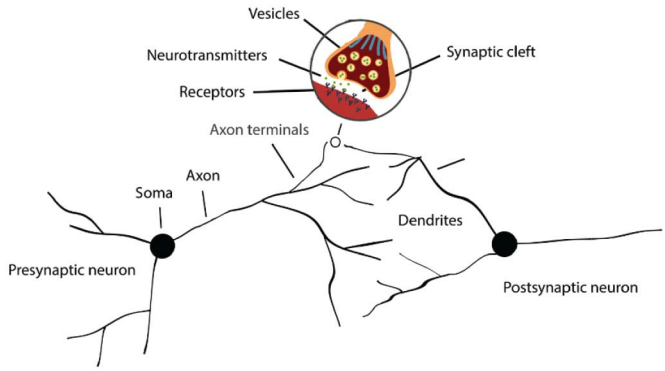

Fig. 1. Biophysical communication between a presynaptic and a postsynaptic neuron.

the specificity of the processing performed by the presynaptic terminals[4].

Specifically, we propose to model the presynaptic terminals of a neuron as an array of transmitters, where each transmitter models the local processing performed by the corresponding presynaptic terminal. We conduct the analysis through a stochastic approach, since the synaptic transmission process is inherently stochastic. More in detail, we first analytically characterize the stochastic filtering of a spike train performed by an arbitrary presynaptic terminal, by showing that the unique and specific processing of a presynaptic terminal can be re-conducted to the cascade of a frequency selector and an amplitude modulator. Then, we characterize the propagation of the presynaptic-filtered signal within the synaptic cleft, by deriving the signal delay as well as the signal attenuation as a function of the distance between the presynaptic transmitter and the postsynaptic receiver.

Finally, the theoretical analysis is validated through numerical simulations, by using a realistic experimentally reconstructed neuron morphology of a mouse, illustrated in Figure 3

The rest of the paper is organized as follows. In Section II, we design the communication engineering model to account for the complex local processing performed by the presynaptic terminals. In Section III, we validate the theoretical analysis. In Section IV, we discuss the derived results, by providing insights on their applicability. Finally, Section V concludes the paper, and some proofs are gathered in the appendix.

II. Presynaptic Terminals: System-Theoretical Model

In this section, we propose a systems-theoretic communication engineering model for capturing the behavior of biological neurons, by accounting for the specificity of the presynaptic-terminal processing. To this aim, we preliminary describe in Section II-A the biophysical mechanisms underlying the compartmentalization at level of the axon terminals of the neuronal processes. Then, in Section II-B we characterize the stochastic filtering performed by each presynaptic terminal. Finally, in Section II-C, we characterize the propagation of the presynaptic-filtered signal within the synaptic cleft.

A. Biophysics of the Axon-Terminal Processing

As mentioned before, experimental studies conducted on biological neurons show a high compartmentalization at level of individual axon terminals of the neuronal processes. This compartmentalization implies that the axon terminals act as independent and dynamic signaling units.

The specificity of the axon-terminal processing is driven by and reflects the complex biophysical mechanisms underlying the release of neurotransmitter-filled vesicles into the synaptic cleft in response to a stimulus. Such mechanisms, that in turn are driven by and reflect the activity history at either or both sides of the synapse [12], [14], [15], have yet to be fully identified and understood. However, experimental studies have revealed that the release of neurotransmitters in response to an AP at a given release site, i.e., at a specialized region of the plasma membrane at which specific proteins involved in the release process are localized, is an extremely complex phenomenon controlled by the wealth and complexity of the protein-protein and protein-lipid interactions. Furthermore, such a complex can vary enormously at the different terminals of an axon under the same conditions [12], [13]. Thus, release sites from a single axon can have different release probabilities, even when the axon contacts the same postsynaptic neuron. The experiments also shown that the release probability is very similar for axon terminals contacting the same dendritic branch of a certain postsynaptic neuron, indicating that the release probability is branch-specific. Specifically, the release probability is not randomly distributed among the axon terminals, but it is rather segregated at the level of individual dendrites, since it reflects the non-uniformity of the dendritic activities [13].

The aforementioned findings justify the following definition, that will be used through the paper.

Definition 1: A *presynaptic terminal*[5] denotes a subset of axon terminals characterized by homogeneous release probability.

B. Presynaptic Terminal Filtering

As previously described and according to experimental evidences, each presynaptic terminal filters independently and in a distinguishing manner the incoming AP sequence. This phenomenon is a consequence of the variations observed in the release probability in different presynaptic terminals, and lead us to propose the systems-theoretic communication model shown in Fig. 2[6]. According to this model, the set of the presynaptic terminals is modeled as an array of transmitters, where each transmitter models the specificity of the stochastic processing performed by a presynaptic terminal. In particular, in

[4]The preliminary version of this work was presented at ACM International Conference on Nanoscale Computing and Communication (ACM NANOCOM 2015) [16].

[5]Although *presynaptic terminal* and *axon terminal* are generally used as synonyms in literature, in the following we adopt Definition 1 to preserve the intuitive meaning evoked by *presynaptic terminal*.

[6]We note that Figure 2 depicts an unique synaptic cleft for the sake of clarity, and the results derived through the paper do not rely on any assumption about a shared molecular channel.

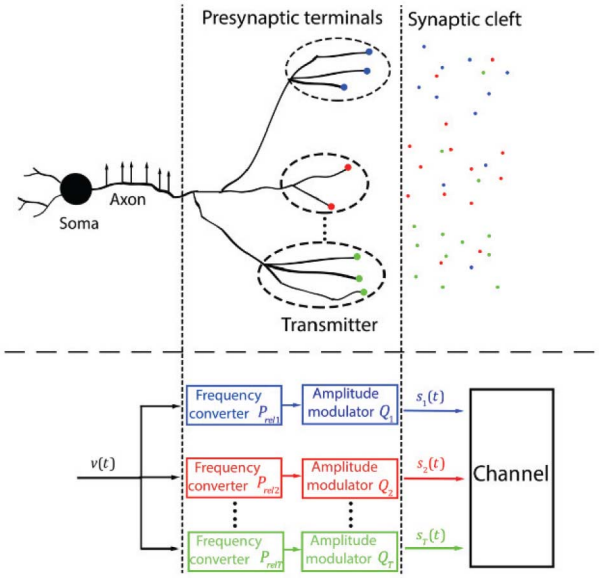

Fig. 2. Transmitter model for the presynaptic terminals.

Proposition 1 and Corollary 1, we prove that such processing can be re-conducted to the cascade of a frequency selector and an amplitude modulator.

The number of the presynaptic terminals and the number of axon terminals constituting a presynaptic terminal depends on the neuron physiology [12], [13]. In the following, without loss of generality, we denote with $\mathcal{T} \triangleq \{1, 2, \ldots, T\}$ the set of distinct presynaptic terminals, whose cardinality is $|\mathcal{T}| = T$, and with n_i the number of axon terminals constituting the i-th presynaptic terminal, with $i \in \mathcal{T}$. In the following, stemming from these definitions, we characterize the input-output relationship of each presynaptic terminal.

The AP train $v(t)$ traveling along the axon of a presynaptic neuron is modeled as a non-homogeneous Poisson impulse process, since this model has been shown to effectively describe the neuron trial-to-trial variability [17]. Specifically, $v(t)$ is equal to:

$$v(t) = \sum_{j=1}^{N(t)} \delta(t - t_j). \tag{1}$$

In (1), t_j is the arbitrary spike arrival time, and $N(t)$ is a non-homogeneous Poisson process whose rate $\lambda(t)$ is a function of the time, hence $E[N(t)] = \int_0^t \lambda(u)du$.

Neurotransmitters are released in the form of packets, quanta. A quantum corresponds to the content of a synaptic vesicle [18] that instantaneously appears in the synaptic cleft. The idealization of the vesicle discharge into the cleft as a point source situated on the presynaptic membrane is a reasonable approximation, since the pore radius though which neurotransmitters are released is negligibly small in comparison with the radius of the synaptic cleft [19].

By definition of presynaptic terminal, it results that a presynaptic terminal release of neurotransmitters corresponds to the neurotransmitter quanta discharged by its axon terminals. We formalize this concept with the following definition:

Definition 2: Q_i denotes the amount of neurotransmitters possibly discharged by the i-th presynaptic terminal in response to an arbitrary AP accounting for the quanta released by the axon terminals constituting the i-th presynaptic terminal:

$$Q_i = \sum_{\ell=1}^{n_i} q_{i,\ell} \tag{2}$$

where $q_{i,\ell}$ is the neurotransmitter quantum discharged by the ℓ-th axon terminal of the i-th presynaptic terminal.

Remark 1: (2) agrees with experimental evidences. In fact, due to the very small size of the axon terminals, each axon terminal is assumed to include a single release site [12]. The number of release sites can therefore be assumed to be equivalent to the number n_i of axon terminals, constituting the arbitrary i-th presynaptic terminal.

According to experimental evidences [12], [13], the axon terminals constituting the i-th presynaptic terminal are characterized by homogeneous physical and chemical properties. Hence, it is reasonable to assume $q_{i,\ell} = q_i, \forall \ell \in \{1, 2, \ldots, n_i\}$, and (2) can be re-write as follows:

$$Q_i = n_i q_i \tag{3}$$

where q_i accounts for the type of neurotransmitters[7] released by the i-th presynaptic terminal. Hence, our model allows each presynaptic terminal to possibly discharge also different types of neurotransmitters, in agreement with neuroscience experiments [12], [14], [15].

Definition 3: $P_{rel_i}(t)$ denotes the release probability of the i-th presynaptic terminal, whose value is determined by the complex interactions between pre- and postsynaptic neurons.

Proposition 1: The signal transmitted by the i-th presynaptic terminal, stimulated by the spike train $v(t)$, is the non-homogenous Poisson impulse process $s_i^v(t)$:

$$s_i^v(t) = Q_i \sum_{j=1}^{N_i(t)} \delta(t - t_j), \tag{4}$$

whose expected value is given by

$$E[s_i^v(t)] = Q_i\, \lambda_i(t) = Q_i\, P_{rel_i}(t)\lambda(t), \tag{5}$$

where Q_i is given by (2) or equivalently by (3) and $\lambda_i(t)$ is the rate of the non-homogenous Poisson process $N_i(t)$ representing the number of releases of the i-th presynaptic terminal until time t:

$$E[N_i(t)] = \int_0^t \lambda_i(u)du = \int_0^t P_{rel_i}(u)\lambda(u)du. \tag{6}$$

Proof: See Appendix A. ■

$s_i^v(t)$ models the neurotransmitter release process at the presynaptic membrane, i.e., it expresses the number of released neurotransmitter molecules as a function of time.

[7] As an example [18], [19], $q_i = 4700$ molecules are released when the neurotransmitter is glutamate,whereas $q_i = 10^4$ molecules are released when the neurotransmitter is acetylcholine. It is worthwhile to note that the type of neurotransmitter impact is not limited to the number of released molecules.

Lemma 1: The probability that the i-th presynaptic terminal emits a non-null signal $s_i^v(t)$ in response to a spike train $v(t)$ goes to zero when the release probability $P_{rel_i}(t)$ goes to zero, regardless of the temporal pattern $\lambda(t)$[8].

Proof: The proof follows directly from Proposition 1. Specifically, when the release probability $P_{rel_i}(t)$ goes to zero, regardless of the frequency pattern $\lambda(t)$ of the incoming stimulus $v(t)$, $s_i^v(t)$ is null identically. In fact, by accounting for (5), its variance (that coincides with the expected value, being $s_i^v(t)$ a non-homogenous Poisson impulse process) and mean are null identically. ■

Remark 2: From Proposition 1 and Lemma 1 and in agreement with experimental evidences [11]–[15], it results that the i-th presynaptic terminal dynamically processes the incoming burst of spikes through: i) its release probability $P_{rel_i}(t)$; ii) the type and quantities of the released neurotransmitters Q_i.

Corollary 1: A presynaptic terminal behaves as a two-stage filter constituted by a frequency converter, controlled by its released probability $P_{rel_i}(t)$, and an amplitude modulator, controlled by Q_i.

Proof: The proof follows directly from Proposition 1. In fact, from (4) and (5), it results that a presynaptic terminal filters the incoming spike train by down-converting the incoming rate through its release probability, i.e., it acts as a frequency converter. Furthermore, a presynaptic terminal modulates the frequency down-converted train in amplitude through Q_i. ■

The results of Proposition 1, Lemma 1 and Corollary 1 are in agreement with experiments conducted in neuroscience. Specifically, the proposed model is able to capture the following observed neuronal phenomena [11]–[15]:

- For a given stimulus $v(t)$, a presynaptic neuron emits different (spatial variable) signals $\{s_i^v(t)\}$ through its different presynaptic terminals. Such signals $\{s_i^v(t)\}$ are characterized by: i) different temporal (frequency) patterns $\{\lambda_i(t)\}_{i\in\mathcal{T}}$; ii) different amplitudes $\{Q_i\}_{i\in\mathcal{T}}$;
- A presynaptic terminal responds differently to stimuli with different temporal patterns $\{\lambda(t)\}$, even if the presynaptic terminal does not change its properties, i.e., $P_{rel_i}(t)$ and Q_i.

Although the molecular interactions underlying the aforementioned neuronal phenomena have yet to be fully identified, the wealth and complexity of the protein-protein and protein-lipid interactions, that have been shown to control the release of neurotransmitters, suggest many ways in which the neurons may modulate the properties of the presynaptic terminals to respond dynamically to different stimuli. In particular, it is widely recognized that these molecular mechanisms are determined by the unique interaction between the pre- and the postsynaptic neurons. Thus, by modulating these biophysical mechanisms, a pre- and a postsynaptic neurons tune the release probabilities along with the type and the quantities of neurotransmitters, determining so the way in which they communicate. In this sense, we can state that the presynaptic terminals constitute a tunable, hence dynamical, transmitter array, where the tuning is determined by the unique interaction between the pre- and postsynaptic neurons. More in detail, "tunable" refers to the experimental evidences according to which changes in the release probability and in the type and quantities of released neurotransmitters represent the main mechanisms by which synaptic efficacy[9] is modulated in neuronal circuits [11]–[15].

Stemming from the above results and comments, we can discern that by tuning the aforementioned quantities a presynaptic neuron: i) selects the postsynaptic neurons to communicate; ii) determines the way it affects its selected postsynaptic neurons. These concepts are illustrated and further investigated in Section IV.

C. Transmission of the Presynaptic Signals

In this subsection, stemming from the above derived results, we characterize the propagation of the signal filtered by the i-th presynaptic terminal within the synaptic cleft. Furthermore, we derive the delay as well as the attenuation a presynaptic signal experiences during the propagation in the synaptic cleft, as a function of the distance between the presynaptic transmitter and the postsynaptic receiver.

Proposition 2: The signal $s_i^v(t)$ transmitted by the i-th presynaptic terminal creates a variation in the neurotransmitter concentration at the m-th postsynaptic dendrite located at a distance d_{im} from the i-th presynaptic terminal given by the following pulse train:

$$\overline{c}_{i,m}(t, d_{im}) = \sum_{j=1}^{N_i(t)} \frac{Q_i}{4\pi a D_i (t - t_j)} e^{-\frac{d_{im}^2}{4D_i(t-t_j)}}, \qquad (7)$$

where D_i is the diffusion coefficient of the synaptic cleft for the neurotransmitter type discharged by the considered presynaptic terminal, and a denotes the width[10] of the synaptic cleft.

Proof: See Appendix B ■

$s_i^v(t)$ models the neurotransmitter release process at the presynaptic membrane, whereas $\overline{c}_{i,m}(t, d_{im})$ models the neurotransmitter concentration at distance d_{im} from the presynaptic membrane, by accounting for the propagation effects introduced by the synaptic cleft. Hence, $\overline{c}_{i,m}(t, d_{im})$ expresses the number of neurotransmitter molecules for volume as a function of time and distance.

Corollary 2: The concentration pulse train $\overline{c}_{i,m}(t, d_{im})$ generated by the i-th presynaptic terminal at the m-th postsynaptic dendrite is a shot-noise process with rate $\lambda_i(t) = P_{rel_i}(t)\lambda(t)$ and with synthetic characterization, i.e., its mean $\mu_{\overline{c}_{i,m}}(t, d_{im}) \triangleq E[\overline{c}_{i,m}(t, d_{im})]$, covariance function $COV_{\overline{c}_{i,m}}(t, \tau, d_{im}) \triangleq E[(\overline{c}_{i,m}(t, d_{im}) - \mu_{\overline{c}_{i,m}}(t, d_{im}))(\overline{c}_{i,m}(t - \tau, d_{im}) - \mu_{\overline{c}_{i,m}}(t - \tau, d_{im}))]$ and variance $\sigma^2_{\overline{c}_{i,m}}(t, d_{im}) \triangleq E[(\overline{c}_{i,m}(t, d_{im}) - \mu_{\overline{c}_{i,m}}(t, d_{im}))^2]$, given by:

[8] In the following, in agreement with the neuroscience literature, we refer to the rate $\lambda(t)$ as the temporal (equivalently, frequency) pattern of the incoming spike train $v(t)$. Similarly, we refer to the rate $\lambda_i(t)$ as the temporal (equivalently, frequency) pattern of the neurotransmitter train released by the i-th presynaptic terminal.

[9] Synaptic efficacy is a basic concept in neuroscience denoting the capacity of a presynaptic input to influence the postsynaptic output [20].

[10] In Section III, we provide the typical physiological quantities of these parameters (a, D_i, and so on) to validate the theoretical analysis.

$$\mu_{\bar{c}_{i,m}}(t, d_{im}) = Q_i \int_{-\infty}^{+\infty} k_{i,m}(t-\tau, d_{im})\lambda(\tau)d\tau = Q_i\, k_{i,m}(t, d_{im}) \otimes \lambda_i(t), \quad (8)$$

$$COV_{\bar{c}_{i,m}}(t, \tau, d_{im}) = Q_i \left[k_{i,m}(t, d_{im})k_{i,m}(t-\tau, d_{im})\right] \otimes \lambda_i(t) = Q_i \int_{-\infty}^{+\infty} k_{i,m}(t-\alpha, d_{im})k_{i,m}(t-\tau-\alpha, d_{im})\lambda_i(\alpha)d\alpha, \quad (9)$$

$$\sigma^2_{\bar{c}_{i,m}}(t, d_{im}) = Q_i \int_{-\infty}^{+\infty} k^2_{i,m}(t-\tau, d_{im})\lambda_i(\tau)d\tau = Q_i\, k^2_{i,m}(t, d_{im}) \otimes \lambda_i(t), \quad (10)$$

where $\otimes$ denotes the convolution operator and $k_{i,m}(t, d_{im}) \triangleq \frac{1}{4\pi a D_i t} e^{-\frac{d^2_{im}}{4D_i t}}$.

Proof: See Appendix C ■

From (8), (9) and (10), it results that the synthetic characterization of $\bar{c}_{i,m}(t, d_{im})$ is a function of both space and time.

Remark 3: From Proposition 2 and Corollary 2 it results that the spatiotemporal variation of the neurotransmitter concentration is a function of: i) the processing of the i-th presynaptic terminal through $P_{rel_i}(t)$ and Q_i; ii) the processing of the channel (synaptic cleft) through $k_{i,m}(t, d_{im})$; iii) the relative position of the receiver (a dendrite of a postsynaptic neuron) through the distance d_{im}.

From Proposition 2 and Corollary 2, it also results that the rate of the concentration train generated by the i-th presynaptic terminal coincides with the rate $\lambda_i(t)$ of the released spike train[11] $s_i^v(t)$. In other words, the temporal patterns of the presynaptic terminals are one-to-one mapped in the temporal patterns of the neurotransmitter concentrations. Since, as experimentally proved [21]–[26], the neuronal information is encoded within the stimulus temporal pattern impinging on a postsynaptic neuron, this result implies that the information carried on the postsynaptic neuron is dictated by the dynamic processing of the presynaptic terminals. This is very important, since it suggests that our model is able to reproduce an experimentally observed phenomenon, i.e, the neuronal information is encoded in the release patterns of the presynaptic terminals [12], [14], [15].

Stemming from the above results, in the following we derive two important metrics of the concentration pulse train, i.e., the concentration delay and the concentration amplitude.

1. Concentration Delay:

Proposition 3: If the i-th presynaptic terminal releases Q_i neurotransmitters at time t_j, the delay t_{im} of the associated concentration pulse needed to reach a postsynaptic membrane located at a distance d_{im} from the i-th presynaptic terminal is given by:

$$t_{im} = t_j + \frac{d^2_{im}}{4D_i}. \quad (11)$$

[11]Clearly, the underlying ligand-binding mechanism at the postsynaptic neuron determines the number of available receptors binding to the released neurotransmitters.

Proof: See Appendix D ■

From (11), it results that the concentration delay is inversely proportional to the diffusion coefficient D_i of the neurotransmitter discharged by the i-th presynaptic terminal. Hence, the higher the diffusion coefficient, the faster the neurotransmitters will propagate. Moreover, the concentration delay is independent of the quantity Q_i of neurotransmitter released by the i-th presynaptic terminal. As future work we plan to further investigate the delay metric, by also accounting for the propagation time of the signal traveling on the axon along with the time spent in the dendritic arbor at the postsynaptic side.

2. Concentration Amplitude: It is also worth to investigate the variation of the concentration amplitude over space, since it can be interpreted as the channel (synaptic cleft) attenuation [27].

Proposition 4: If the i-th presynaptic terminal releases Q_i neurotransmitters in the synaptic cleft, the concentration pulse is attenuated by the channel according to a quadratic low of the distance d from the i-th presynaptic terminal:

$$a_i(Q_i, d) = \pi\, a\, e \frac{d^2}{Q_i}. \quad (12)$$

Proof: The synaptic cleft attenuation can be determined by evaluating the inverse of the amplitude of the concentration pulse at the time instant at which the concentration pulse reaches its maximum value [27], which we have previously determined in Proposition 3. Hence, by substituting (11) in $Q_i k_{i,m}(t - t_j, d_{im})$ given in (17) (Appendix B), the proof follows. ■

It is interesting to note that, the higher the quantity of released neurotransmitters Q_i, the smaller the channel attenuation, as in the classical amplitude modulation. Moreover, we note that the attenuation is independent of the neurotransmitter diffusion coefficient, differently from the concentration delay. Specifically, the diffusion coefficient of the synaptic cleft for the type of neurotransmitters discharged by the i-the presynaptic terminal does not affect the attenuation of the neurotransmitters throughout the space.

Remark 4: As detailed discussed in Section IV, the long term goal is to enable implantable nanomachines able to substitute damaged neurons. To this aim, the nanomachines have to be able not only to sense the normal neuron activities but also to mimic the behavior of biological neurons. Hence, the knowledge of the variation of the neurotransmitters concentration amplitude over space along with the delay experienced is crucial for achieving such a long term goal.

III. Validation of the Theoretical Results

In this section, we validate the theoretical results through simulations. Specifically, we use the realistic experimentally reconstructed mouse neuron morphology "NMO-07522" [28] released by NeuroMorpho.org archive. The neuron morphology is shown in Fig. 3. The considered neuron exhibits two different presynaptic terminals, since, as described in Section II, it is possible to individuate two different homogeneous release zones contacting two different dendritic branches. The release

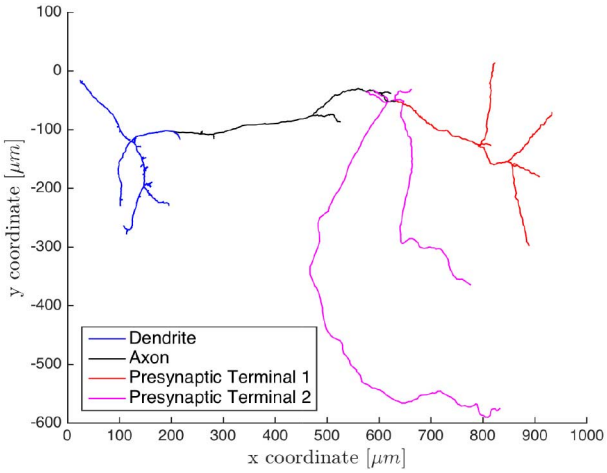

Fig. 3. NMO-07522 neuron morphology with two presynaptic terminals.

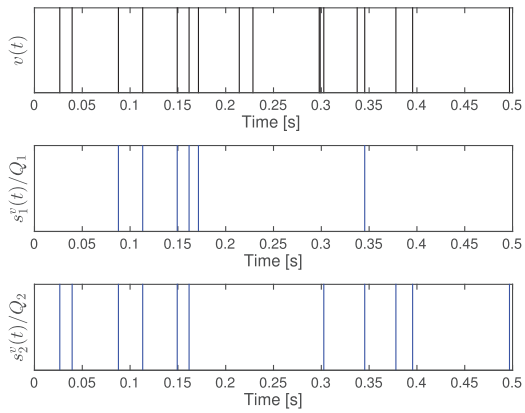

Fig. 4. Frequency-conversion processing of the presynaptic terminals.

probabilities of the two presynaptic terminals are equal to $P_{rel_1} = 0.3$ and $P_{rel_2} = 0.7$ according to [13].

In Fig. 4, we report the responses $s_1^v(t)$ and $s_2^v(t)$ of the two presynaptic terminals when they are stimulated by a non-homogeneous Poisson AP train $v(t)$ with a sinusoidal rate whose average values is 32Hz [29]. We note that the first presynaptic terminal, characterized by a lower release probability, generates a signal $s_1^v(t)$ whose rate is lower than the one of $s_2^v(t)$, generated by the second presynaptic terminal, characterized by a larger release probability. These results are in agreement with the theoretical analysis, since they confirm that the presynaptic terminals perform frequency conversions of the incoming spike train through their release probabilities.

In Fig. 5, we report the rate $\lambda_1(t)$ of the signal $s_1^v(t)$ emitted by the first presynaptic terminal, by taking the same simulation setting of the previous experiment. The results validate the analysis developed in Section II, confirming that the rate of the signal emitted by a presynaptic terminal is the modulated version of the rate of the incoming spike train through its release probability, i.e., $\lambda_i(t) = P_{rel_i}(t)\lambda(t)$.

In Fig. 6, we simulate the vesicle releases at both the considered presynaptic terminals over 5 trials for the stimulus train $v(t)$ used in the first experiment (Fig. 4). Specifically, the vesicle releases are indicated by the blue dots. As expected, the

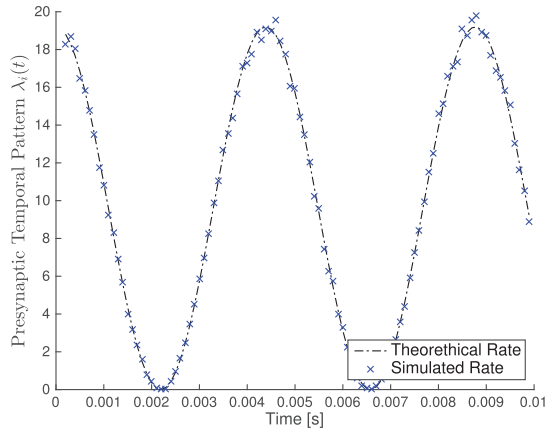

Fig. 5 Presynaptic terminal temporal pattern $\lambda_i(t)$ vs time. Y-coordinate expressed in releases per second.

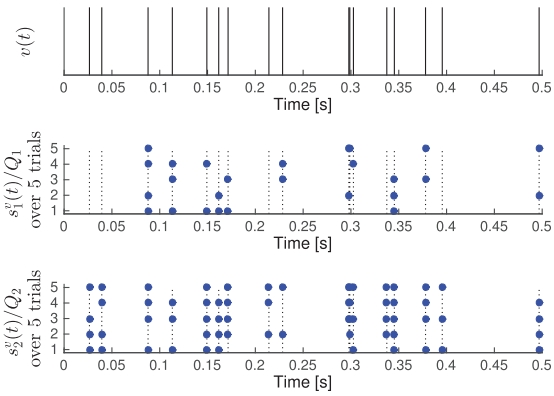

Fig. 6. Vesicle releases over 5 trials for both the considered presynaptic terminals. Release events shown with blue dots.

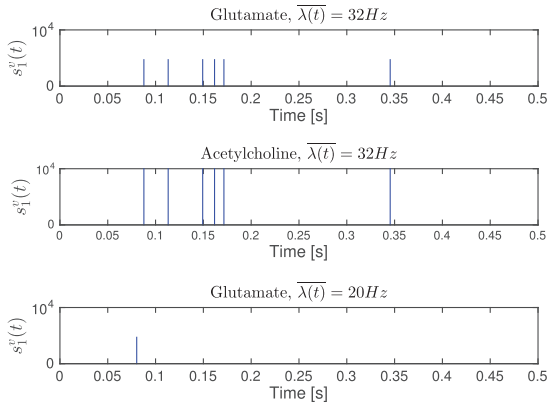

Fig. 7. Amplitude modulation processing of the presynaptic terminals. Y-coordinate expressed in number of molecules.

number of vesicle releases for the first presynaptic terminal, characterized by a lower release probability, is smaller than the number of release for the second presynaptic terminal, for all the considered trials. This variability in the neurotransmitter releases confers the specificity to the presynaptic processing.

In Fig. 7, we simulate the response $s_1^v(t)$ of the first presynaptic terminal when it emits two different kind of neurotransmitters, i.e., glutamate and acetylcholine. The number of molecules is assumed equal to $Q_1 = 4700$ and $Q_1 = 10^4$, respectively, as

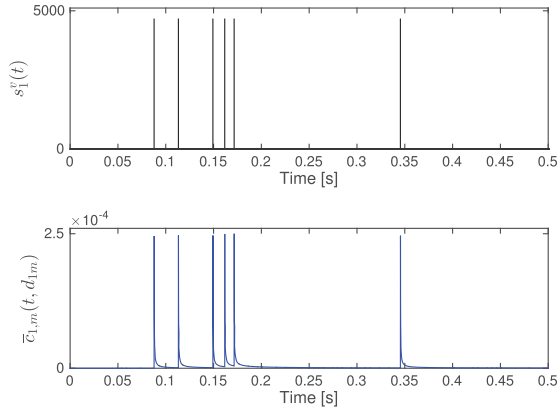

Fig. 8. Concentration pulse train due to the first presynaptic terminal. Y-coordinate expressed in molecules per nm^3 (second plot).

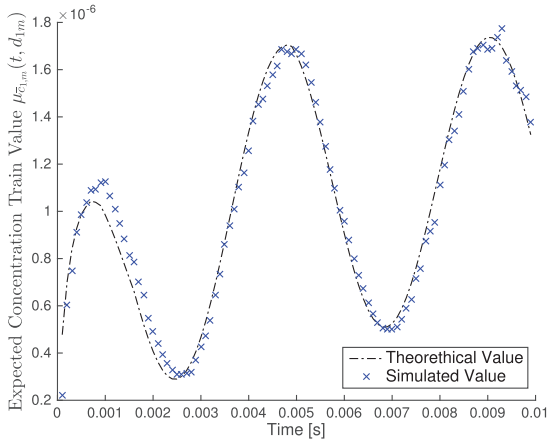

Fig. 9. Expected value of the concentration pulse train vs time. Y-coordinate expressed in molecules per nm^3.

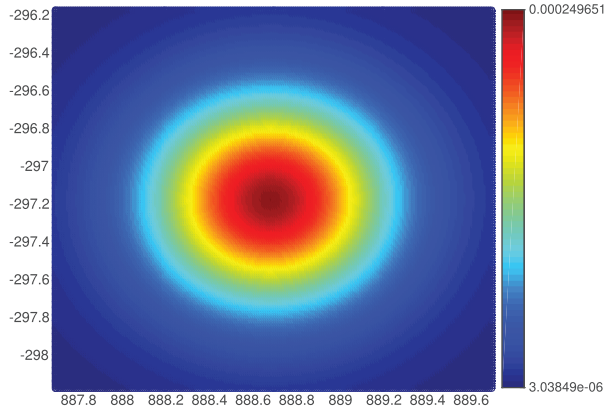

Fig. 10. Concentration vs space for the first presynaptic terminal at time $t = 0.1618$. X- and Y-coordinates expressed in nm and Z-coordinate (color map) expressed in molecules per nm^3.

reported in [18], [19]. In the first experiment, we assume that the presynaptic terminal is stimulated by a non-homogeneous Poisson AP train $v(t)$ with a sinusoidal rate $\lambda(t)$ whose average value is 32Hz. By comparing the first and the second plot reported in Fig. 7, we note that for the acetylcholine the presynaptic response has a larger strength, since the number of emitted neurotransmitters is larger. These results are in agreement with the theoretical analysis, since they confirm that the presynaptic terminals perform an amplitude modulation of the incoming spike train through the type and quantities of the released neurotransmitters. In the second experiment, we stimulate the first presynaptic terminal with a non-homogeneous Poisson AP train $v(t)$ with a different sinusoidal rate $\lambda(t)$, having average value equal to 20Hz, when $Q_1 = 4700$. By comparing the first and the third plot reported in Fig. 7, the theoretical analysis is again confirmed. In fact, the presynaptic terminal responds differently to stimuli with different temporal patterns, even though the release probability and the type and number of neurotransmitters do not change.

In Fig. 8, we report the concentration pulse train $\bar{c}_{1,m}(t, d_{1m})$ generated at distance $d_{1m} = 20$nm by the signal $s_1^v(t)$ emitted by the first presynaptic terminal as a function of the time. We adopt the same simulation setting described in [18] where glutamate is the neurotransmitter, i.e., $Q_1 = 4700$ molecules, $D_1 = 7.6 \cdot 10^8 nm^2/s$ and $a = 20nm$. We note that the results confirm the theoretical analysis, i.e., the neuronal information is encoded in the release patterns of the presynaptic terminals. In fact, the rate of the concentration pulse train generated by the first presynaptic terminal coincides with the rate of the released spike, i.e., $\lambda_1(t) = P_{rel_1}(t)\lambda(t)$. Hence the temporal patterns of the presynaptic terminals are commutated in the temporal patterns of the neurotransmitter concentrations. We also underline that the delay experienced by the signal through the channel is neglectful for the assumed parameter setting, hence it cannot be properly visualized.

Furthermore, in Fig. 9 we report the expected value $\mu_{\bar{c}_{1,m}}(t, d_{1m})$ of the concentration train generated at distance of $d_{1m} = 20$nm by the signal $s_1^v(t)$ emitted by the first presynaptic terminal as a function of the time. The results validate once again the theoretical analysis developed in Section II. In fact, the simulated expected value of the concentration train matches very well the theoretical one given in equation (8).

In Fig. 10, we report the instantaneous concentration value $\bar{c}_{1,m}(t, d_{1m})$ of the neurotransmitters released by the first presynaptic terminal as a function of the space. We plot the values at the time instant $t = 0.1618$s, i.e., $100\mu s$ after a release event (see Fig. 8), and the results confirm the impulsive nature of the concentration, which decreases of two orders of magnitude within a distance of the order of the μm.

Finally, in Fig. 11, we report the concentration pulse train $\bar{c}_{2,m}(t, d_{2m})$ generated at distance $d_{2m} = 20$nm by the signal $s_2^v(t)$ emitted by the second presynaptic terminal as function of the time. We adopt the same simulation setting described above, and all the previous consideration continue to hold. Furthermore, since the processing performed by the second presynaptic terminal is different from the one performed by the first presynaptic terminal, the concentration pulse train is different.

IV. Discussion

Here we conduct a brief discussion stemming from the results derived through the paper. Our theoretical analysis has

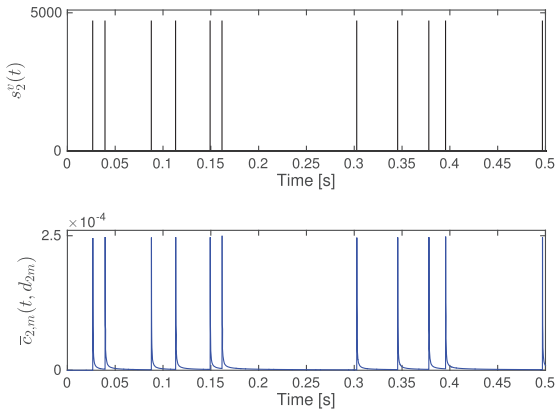

Fig. 11. Concentration pulse train due to the second presynaptic terminal. Y-coordinate expressed in molecules per nm^3 (second plot).

proved that the unique and specific processing of a presynaptic terminal can be re-conducted to the cascade of a frequency selector and an amplitude modulator. More in detail, in agreement with experimental evidences [11]–[15], we design a communication engineering model where:

- For a given stimulus $v(t)$, a presynaptic neuron emits different (spatial variable) signals $s_i^v(t)$ through its different presynaptic terminals. These signals can differ: i) in amplitude through Q_i; ii) in the temporal pattern $\lambda_i(t)$ through $P_{rel_i}(t)$. In other words, a presynaptic neuron produces spatial-frequency variable signals for a given stimulus through the dynamics filtering of its presynaptic terminals.
- A presynaptic terminal responds differently to stimuli characterized by different patterns $\lambda(t)$, even if the presynaptic terminal does not change its properties, i.e., $P_{rel_i}(t)$ and Q_i.
- The information transmitted to the postsynaptic neuron is dictated by the dynamic processing of the presynaptic terminals, since the neuronal information is encoded in the release patterns of the presynaptic terminals.

The proposed engineering model represents a first step toward the design of radically new medical diagnosis and treatment techniques based on the deployment of nanomachines inside the nervous system. As instance, let us consider a brain disease caused by a failure event in the propagation of the neuronal signals [8], [30]. In such a case, it is possible to envision nanomachines implanted in the brain to seamlessly substitute damaged neurons and their interconnections, by repairing so the lost functionalities of damaged neurons. For this, the implanted nanomachines need to: i) sense the electrochemical activity patterns coming from the healthy neurons; ii) process these patterns by emulating the healthy neuronal process of the neurons they substitute; iii) induce the corresponding output pattern to the next healthy neuron. It is clear that many questions and challenges must be addressed before a system that leverages the above attributes could become a reality. Nevertheless, models providing an engineering abstraction of the behavior of healthy biological neurons, as the one proposed within the manuscript, constitute the first step in such a direction.

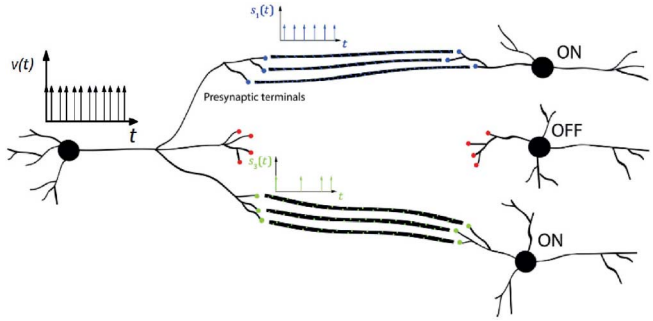

Fig. 12. The tuning of the temporal patterns and the strengths of the presynaptic terminal releases selects the neurons to communicate.

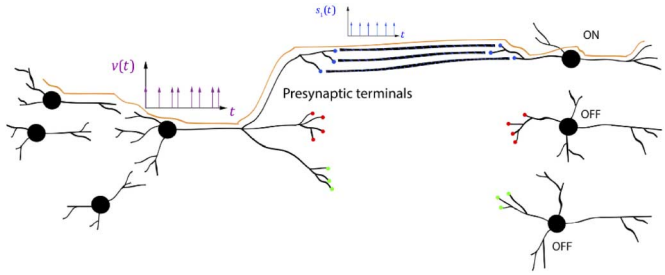

Fig. 13. Neurons select the information route through dynamical spatial-frequency filtering.

Further insights for the design of future intrabody nanonetworks can be drawn by combining the results derived within the manuscript with the existing literature. Specifically, experimental data [21]–[26], recently formalized with a system-theoretical model in [10], have proved that a postsynaptic neuron filters the stimuli impinging on its spatial distributed dendrites according to their temporal patterns. Hence, the communication among neurons is spatial-frequency selective, i.e., a stimulus with a certain temporal pattern can activate the response of a postsynaptic neuron and it can not activate the response of another postsynaptic neuron. By combining these results with the ones derived within the manuscript, we can state, as shown in Fig. 12, that a presynaptic neuron:

- *selects* the postsynaptic neurons to communicate with through the temporal patterns of its releases, i.e., through a proper tuning of $\{P_{rel_i}(t)\}_{i \in \mathcal{T}}$;
- *determines* the way it affects its postsynaptic neurons through an amplitude modulation, i.e., through a proper tuning of Q_i.

In a nutshell, neurons select the "route" the information has to follow through dynamical spatial-frequency filtering, as illustrated in Fig. 13. Such a behavior could be exploited for the implementation of novel communication techniques between the nanomachines and/or between nanomachines and biological neurons, along with controlling strategies of network topology and connectivity. Specifically, a nanomachine could force a neuronal response by properly selecting the frequency content of its emitted signal. Moreover, a nanomachine could limit the possible interference generated on the normal neuronal activities by exploiting the spatial-frequency selectivity of the surrounding neurons. As future works, we plan to further investigate such a crucial aspect.

V. Conclusion

In this paper, we proposed a transmitter model for capturing the behavior of biological neurons, by accounting for compartmentalization at the level of the presynaptic terminals of the neuronal processing, induced by the variability of the release probability within the presynaptic terminals. Specifically, we have modeled the presynaptic terminals as a tunable transmitter array, with each transmitter characterizing the stochastic filtering performed by a presynaptic terminal. We have shown that the unique and specific processing of a presynaptic terminal can be re-conducted to the cascade of a frequency selector and an amplitude modulator. This result is crucial for the development of future intrabody nanonetwork applications based on the deployment of nanomachines inside the nervous system, as for example radically new medical diagnosis and treatment techniques. In fact, such a result provides an engineering abstraction of the neuronal processes to be used in the design of the artificial nanomachines for intrabody nanonetworks. We will further investigate such a topic as future research direction.

Appendix A
Proof of Proposition 1

Let us denote with R_i the subset of the spike arrival times $\{t_j\}_{j=1}^{N(t)}$ that produce the release of neurotransmitters at the i-th presynaptic terminal. Stemming from this and accounting for Definition 2, with reference to the k-th AP of the incoming train, the signal $s_i(t)$ at the output of the i-th presynaptic terminal is given by:

$$s_i(t) = Q_i \delta(t - t_k) \mathbf{1}_{R_i}(t_k), \tag{13}$$

where $\mathbf{1}_{R_i}(\cdot)$ is the indicator function of R_i, defined as:

$$\mathbf{1}_{R_i}(t_k) = \begin{cases} 1, & \text{if } t_k \in R_i \\ 0, & \text{if } t_k \notin R_i. \end{cases} \tag{14}$$

By accounting for (13) and (1), it results that the response of the i-th presynaptic terminal to the spike train $v(t)$ is:

$$s_i^v(t) = Q_i \sum_{k=1}^{N(t)} \delta(t - t_k) \mathbf{1}_{R_i}(t_k) = Q_i \sum_{j=1}^{N_i(t)} \delta(t - t_j), \tag{15}$$

where Q_i is given by (2) or equivalently by (3), and $N_i(t)$ is the stochastic process representing the number of releases of the i-th presynaptic terminal until time t. The stochastic process in (15) is a thinned process [31], that according to the neuroscience experimental evidences, can be modeled as a non-homogenous Poisson impulse process [17], [32], whose rate is given by[12]:

$$\lambda_i(t) = P_{rel_i}(t) \lambda(t). \tag{16}$$

Hence the proof follows by recalling that the expected value of a non-homogenous Poisson impulse process is $E[s_i^v(t)] = Q_i \, \lambda_i(t) = Q_i \, P_{rel_i}(t) \lambda(t)$, and that the expected value of $N_i(t)$ is $E[N_i(t)] = \int_0^t \lambda_i(u) du = \int_0^t P_{rel_i}(u) \lambda(u) du$.

[12]The release is assumed to occur only when a spike invades the presynaptic terminal, i.e., the spontaneous release probability is assumed to be zero [11].

Appendix B
Proof of Proposition 2

When a neurotransmitter quantum is released, it propagates throughout the synaptic cleft. Its propagation can be analytically modeled by solving the Fick's laws of the diffusion for a two-dimensional disc [18], [19]. Hence, by accounting for (13), if at t_j, Q_i neurotransmitters are released from the i-th presynaptic terminal, the concentration at the m-th postsynaptic dendrite located at a distance d_{im} from the i-th presynaptic terminal as a function of time t is [18], [19] :

$$c_{i,m}(t, d_{im}) = \frac{Q_i}{4\pi a D_i (t - t_j)} e^{-\frac{d_{im}^2}{4D_i(t-t_j)}}, \tag{17}$$

By exploiting (4), the proof follows.

Appendix C
Proof of Corollary 2

By defining $k_{i,m}(t, d_{im}) \triangleq \frac{1}{4\pi a D_i t} e^{-\frac{d_{im}^2}{4D_i t}}$ and by exploiting (4), the concentration train given in (7) can be re-written as

$$\overline{c}_{i,m}(t, d_{im}) = s_i^v(t) \otimes k_{i,m}(t, d_{im}) = Q_i \sum_{j=1}^{N_i(t)} k_{i,m}(t - t_j, d_{im}). \tag{18}$$

(18) is a shot-noise process [33], being $s_i^v(t)$ a point Poisson process. Hence, by accounting for the generalized Campbells' Theorem [33], we can derive its synthetic characterization as in (8), (9) and (10), and the proof follows.

Appendix D
Proof of Proposition 3

To derive the delay with which a neurotransmitter concentration pulse arrives at the m-th postsynaptic dendrite located at a distance d_{im} from the i-th presynaptic terminal, we compute the time instant at which $Q_i k_{i,m}(t - t_j, d_{im})$ given in (17) reaches its global maximum [27]. In fact, $Q_i k_{i,m}(t - t_j, d_{im})$ has only one local maximum, which is also its global maximum. We can therefore compute the position of this maximum by taking the time derivative of the pulse equation and finding the time instant at which it is equal to zero:

$$\frac{d\{Q_i k_{i,m}(t - t_j, d_{im})\}}{dt} = \frac{d}{dt} \frac{Q_i e^{-\frac{d_{im}^2}{4D_i(t-t_j)}}}{4\pi a D_i (t - t_j)} = 0. \tag{19}$$

From (19), by isolating the variable t, with some algebraic manipulations, one obtains:

$$t_{im} = t_j + \frac{d_{im}^2}{4D_i}. \tag{20}$$

This time t_{im} can be interpreted as the time the concentration pulse spends to reach the postsynaptic membrane located at a distance r_{im} from the i-th presynaptic terminal if the neurotransmitter quantum was released at t_j, i.e., t_{im} can be interpreted as the delay, and the proof follows.

REFERENCES

[1] I. F. Akyildiz, J. M. Jornet, and M. Pierobon, "Nanonetworks: A new frontier in communications," *ACM Commun.*, vol. 54, no. 11, pp. 84–89, Nov. 2011.

[2] J. M. Jornet and I. F. Akyildiz, "Graphene-based plasmonic nano-antenna for terahertz band communication in nanonetworks," *IEEE J. Sel. Areas Commun.*, vol. 31, no. 12, pp. 685–694, Dec. 2013.

[3] D. Malak and O. B. Akan, "Molecular communication nanonetworks inside human body," *Nano Commun. Netw.*, vol. 3, no. 1, pp. 19–35, 2012.

[4] G. Santagati and T. Melodia, "Opto-ultrasonic communications in wireless body area nanonetworks," in *Proc. Asilomar Conf. Signals Syst. Comput.*, no. 2013, pp. 1066–1070.

[5] S. Balasubramaniam *et al.*, "Development of artificial neuronal networks for molecular communication," *Nano Commun. Netw.*, vol. 2, nos. 2–3, pp. 150–160, 2011.

[6] D. Seo, J. M. Carmena, E. A. Jan, M. Rabaey, and M. M. Maharbiz, "Neural dust: An ultrasonic, low power solution for chronic brain-machine interfaces," arxiv.org/abs/1307.2196, Jul. 2013.

[7] J. Suzuki, S. Balasubramaniam, S. Pautot, V. D. P Meza, and Y. Koucheryavy, "A service-oriented architecture for body area nanonetworks with neuron-based molecular communication," *Mobile Netw. Appl.*, vol. 19, no. 6, pp. 707–717, 2014.

[8] M. Veletic, P. A. Floor, and I. Balasingham, "From nano-scale neural excitability to long term synaptic modification," in *Proc. ACM NanoCom*, May 2014, pp. 1–8.

[9] D. Malak and O. Akan, "Communication theoretical understanding of intra-body nervous nanonetworks," *IEEE Commun. Mag.*, vol. 52, no. 4, pp. 129–135, Apr. 2014.

[10] A. S. Cacciapuoti and M. Caleffi, "Receiver design for a bionic nervous system: Modeling the dendritic processing power," *IEEE Internet Things J.*, vol. 3, no. 1, pp. 27–37, Feb. 2016.

[11] W. Maass and A. M. Zador, "Dynamic stochastic synapses as computational units," *Neural Comput.*, vol. 11, no. 4, pp. 903–911, 1999.

[12] A. M. Thomson, "Presynaptic frequency-and pattern-dependent filtering," *J Comput. Neurosci.*, vol. 15, no. 2, pp. 159–202, 2003.

[13] T. Branco, K. Staras, K. J. Darcy, and Y. Goda, "Local dendritic activity sets release probability at hippocampal synapses," *Neuron*, vol. 59, no. 3, pp. 475–485, 2008.

[14] L. F. Abbott and W. G. Regehr, "Synaptic computation," *Nature*, vol. 431, pp. 796–803, Oct. 2004.

[15] H. Markram, A. Gupta, A. Uziel, Y. Wang, and M. Tsodyks, "Information processing with frequency-dependent synaptic connections," *Neurobiol. Learn. Memory*, vol. 70, nos. 1–2, pp. 101–112, 1998.

[16] A. S. Cacciapuoti, M. Caleffi, and A. Piras, "Neuronal communication: Presynaptic terminals as transmitter array," in *Proc. ACM NANOCOM*, 2015, pp. 12:1–12:5.

[17] M. V. Tsodyks and H. Markram, "The neural code between neocortical pyramidal neurons depends on neurotransmitter release probability," *Proc. Nat. Acad. Sci.*, 1997, vol. 94, no. 2, pp. 719–723.

[18] B. Barbour and M. Hausser, "Intersynaptic diffusion of neurotransmitter," *Trends Neurosci.*, vol. 20, no. 9, pp. 377–384, 1997.

[19] R. Khanin, H. Parnas, and L. Segel, "Diffusion cannot govern the discharge of neurotransmitter in fast synapses," *Biophys. J.*, vol. 67, no. 3, pp. 966–972, 1994.

[20] J. C. Lopez, "Computational neuroscience: Quantifying synaptic efficacy," *Nat. Rev. Neurosci.*, vol. 3, no. 332, pp. 332, 2002.

[21] J. Laudanski, B. Torben-Nielsen, I. Segev, and S. Shamma, "Spatially distributed dendritic resonance selectively filters synaptic input," *PLoS Comput. Biol.*, vol. 10, no. 8, pp. 1–10, Aug. 2014.

[22] T. Branco and M. Hausser, "The single dendritic branch as a fundamental functional unit in the nervous system," *Curr. Opin. Neurobiol.*, vol. 20, no. 4, pp. 494–502, 2010.

[23] A. Polsky, B. Mel, and J. Schiller, "Computational subunits in thin dendrites of pyramidal cells," *Nat. Neurosci.*, vol. 9, no. 3, pp. 206–221, Mar. 2008.

[24] C. Koch, T. Poggio, and V. Torres, "Retinal ganglion cells: A functional interpretation of dendritic morphology," *Philos. Trans. R. Soc. London B Biol. Sci.*, vol. 298, no. 1090, pp. 227–263, 1982.

[25] E. M. Izhikevich and E. C. W. N. S. Desai, "Bursts as a unit of neural information: Selective communication via resonance," *Trends Neurosci.*, vol. 26, no. 3, pp. 161–167, 2003.

[26] B. Hutcheon and Y. Yarom, "Resonance, oscillation and the intrinsic frequency preferences of neurons," *Trends Neurosci.*, vol. 23, no. 5, pp. 216–222, 2000.

[27] I. Llatser, A. Cabellos-Aparicio, M. Pierobon, and E. Alarcon, "Detection techniques for diffusion-based molecular communication," *IEEE J. Sel. Areas Commun.*, vol. 31, no. 12, pp. 726–734, Dec. 2013.

[28] B. A. Sava *et al.*, "Electrophysiological and morphological properties of Cajal-Retzius cells with different ontogenetic origins," *Neuroscience*, vol. 167, no. 3, pp. 724–734, 2010.

[29] M. Siegel, M. R. Warden, and E. K. Miller, "Phase-dependent neuronal coding of objects in short-term memory," *Proc. Nat. Acad. Sci.*, 2009, vol. 106, no. 50, pp. 21341–21346.

[30] F. Mesiti and I. Balasingham, "Nanomachine-to-neuron communication interfaces for neuronal stimulation at nanoscale," *IEEE J. Sel. Areas Commun.*, vol. 31, no. 12, pp. 695–704, Dec. 2013.

[31] R. L. Streit, *Poisson Point Processes*. New York, NY, USA: Springer, 2010.

[32] D. Heeger, "Poisson model of spike generation," Univ. Standford, 2000.

[33] A. Papoulis, *Probability, Random Variables, and Stochastic Processes*. New York, NY, USA: McGraw-Hill, 1984.

Angela Sara Cacciapuoti (M'10–SM'16) received the Dr. Eng. degree (*summa cum laude*) in telecommunications engineering, and the Ph.D. degree (with score "excellent") in electronic and telecommunications engineering, both from University of Naples Federico II, in 2005 and 2009, respectively. Currently, she is an Assistant Professor with DIETI Department, University of Naples Federico II, Naples, Italy. Since 2014, she is an Area Editor of *Computer Networks* (Elsevier). From 2010 to 2011, she has been with the Broadband Wireless Networking Laboratory, Georgia Institute of Technology, Atlanta, GA, USA, as a Visiting Researcher. In 2011, she has also been with the NaNoNetworking Center in Catalunya (N3Cat), Universitat PolitËcnica de Catalunya (UPC), Barcelona, Spain, as a Visiting Researcher. Her research interests include cognitive radio networks, nanonetworks, neuronal models, and Internet of Nano-Things.

Marcello Caleffi (M'12–SM'16) received the Dr.Eng. degree (*summa cum laude*) in computer science engineering from the University of Lecce, Lecce, Italy, in 2005, and the Ph.D. degree in electronic and telecommunications engineering from the University of Naples Federico II, Naples, Italy, in 2009. Currently, he is an Assistant Professor with DIETI Department, University of Naples Federico II, where he teaches telematics and mobile communication systems classes and supervised and graduated more than 20 B.S. and M.S. students. From 2010 to 2011, he was with the Broadband Wireless Networking Laboratory, Georgia Institute of Technology, Atlanta, GA, USA, as a Visiting Researcher. In 2011, he was also with the NaNoNetworking Center in Catalunya (N3Cat), Universitat PolitËcnica de Catalunya (UPC), Barcelona, Spain, as a Visiting Researcher. His research interests include cognitive radio networks, biological networks, and nanonetworks, and he has coauthored over 40 journal (the IEEE ACM TRANSACTION ON NETWORKING, the IEEE TRANSACTION ON WIRELESS COMMUNICATIONS, the IEEE TRANSACTION ON COMMUNICATIONS, the IEEE TRANSACTION ON VEHICULAR TECHNOLOGY, and the IEEE INTERNET OF THINGS JOURNAL) and conference (the IEEE GLOBECOM, the IEEE ICC, the IEEE SECON, ACM NANOCOM) publications. Since 2014, Marcello Caleffi serves as an Area Editor for *Ad Hoc Networks* (Elsevier).

Alessandro Piras received the master's degree in electronic engineering from the Second University of Naples, Caserta, Italy, on March 2014. Since 2015, he has been a Research Fellow with the Consorzio Nazionale Interuniversitario per le Telecomunicazioni (CNIT). His research interests include nanonetworks and computational neuroscience.